A Qualitative Study of the Damped Duffing Equation and Applications[1]

Zhaosheng Feng[2]

Department of Mathematics, University of Texas-Pan American, Edinburg, TX 78541

Goong Chen[3]

Department of Mathematics, Texas A&M University, College Station, TX 77843

Sze-Bi Hsu[4]

Department of Mathematics, National Tsing Hua University, Hsinchu, 30043, Taiwan, R.O.C.

Abstract. In this paper, we analyze the damped Duffing equation by means of qualitative theory of planar systems. Under certain parametric choices, the global structure in the Poincaré phase plane of an equivalent two-dimensional autonomous system is plotted. Exact solutions are obtained by using the Lie symmetry and the coordinate transformation method, respectively. Applications of the second approach to some nonlinear evolution equations such as the two-dimensional dissipative Klein-Gordon equation are illustrated.

Keywords: Duffing's equation, autonomous system, phase plane, global structure, equilibrium point, Lie symmetry.

AMS (MOS) Subject Classification: 34C05, 34C14, 34C20, 35B40.

1 Introduction

Many physical phenomena are modeled by nonlinear systems of ordinary differential equations. An important problem in the study of nonlinear systems is to find exact solutions and explicitly describe traveling wave behaviors. Modern theories describe traveling waves and coherent structures in many fields, including general relativity, high energy particle physics, plasmas, atmosphere and oceans, animal dispersal, random media, chemical reactions, biology, nonlinear electrical circuits, and nonlinear optics. For example, in nonlinear optics, the mathematics developed for the propagation of information via optical solitons is quite striking,

---

[1]The work is supported by UTPA Faculty Research Council Grant 119100.

[2]Corresponding author: zsfeng@utpa.edu; Fax: (956) 384-5091.

[3]E-mail: gchen@math.tamu.edu; Fax: (979) 862-4190.

[4]E-mail: sbhsu@math.nthu.edu.tw.

with extremely high accuracy. It has been experimentally verified, with a span of twelve orders of magnitude: from the wavelength of light to transoceanic distances. It also guides the practical applications in modern telecommunications. Many other nonlinear wave theories mentioned above have also achieved similar success.

Motivated by potential applications in physics, engineering, biology and communication theory, the damped Duffing equation

$$\ddot{x} + \delta \dot{x} - \mu x + x^3 = 0, \tag{1.1}$$

has received wide interest. In the above, δ is the coefficient of viscous damping and the term $-\mu x + x^3$ represents the nonlinear restoring force, acting like a hard spring, and the dot denotes differentiation with respect to time. Equation (1.1) is a ubiquitous model arising in many branches of physics and engineering such as the study of oscillations of a rigid pendulum undergoing with moderately large amplitude motion [1], vibrations of a buckled beam, and so on [2-4]. It has provided a useful paradigm for studying nonlinear oscillations and chaotic dynamical systems, dating back to the development of approximate analytical methods based on perturbative ideas [1], and continuing with the advent of fast numerical integration by computer, to be used as an archetypal illustration of chaos [2, 4-7]. Various methods for studying the damped Duffing equation and the forced Duffing equation in feedback control [8-11], strange attractor [12-16], stability [17-19], periodic solutions [20-23] and numerical simulations [24-26], etc., have been proposed and a vast number of profound results have been established. A phase plane analysis of the Duffing equation can be seen in [27] and more qualitative studies have been described in [28]. Exact solutions were discussed by Chen [29] using the target function method, but no explicit solutions were shown. Note that equation (1.1) satisfies the Painlevé condition with a certain parametric choice [30, 31]. In [32], exact solutions were presented by using the elliptic function method for various special cases. Senthil and Lakshmanan [33] dealt with equation (1.1) by using the Lie symmetry method and derived an exact solution from the properties of the symmetry vector fields. Harmonic solutions were investigated by McCartin using the method of van der Pol [17]. The behavior of the solutions of the Duffing equation near the separatrix were treated by Hale and Spezamiglio [34].

There is another problem source. Many nonlinear partial differential systems can be converted into nonlinear ordinary differential equations (ODEs) after making traveling wave transformations. Seeking traveling wave solutions for those nonlinear systems is somehow equivalent to finding exact solutions of corresponding ODEs. A typical example is the 2D dissipative Klein-Gordon equation which arises in relativistic quantum mechanics [35, 36]

$$u_{tt} - \Delta u + \alpha u_t + \beta u + \gamma u^3 = 0, \tag{1.2}$$

where α, β and γ are real physical constants. When $\alpha = 0$, the Kelin-Gordon equation plays a fundamental role as a model equation in nonlinear field theories [37, 38], lattice dynamics [39] and nonlinear optics [40]. Stationary baseband solutions of the equation come about as a balance between nonlinearity and dispersion, and thus represent solitary wave solutions to the system. While analytic solutions in powers of sech functions can be determined in one dimension [41], radially symmetric higher-dimensional solutions may not have simple analytic form; the analysis for these solutions are thus dominated by numerical methods and variational techniques [42-43, etc.]. Recently, a considerable number of papers have appeared to various aspects of equation (1.1): the identification problems was investigated by Ha and Nakagiri et al. using the transposition method [44-46]; the global existence and the asymptotic behavior of solutions were undertook by Kosecki et al [47-49]; the uniqueness of a time-periodic solution was proved by Gao and Guo using the Galerkin method as well as Leray-Schauder fixed point theorem [50]; approximate solutions and solitons trapping for the nonlinear Klein-Gordon equation with quadratic and cubic nonlinearities were studied by Maccari using the asymptotic perturbation method [51].

Notably, equations (1.1) and (1.2) are *not integrable* in the general case. Therefore, to analyze their solutions, a qualitative study together with innovative mathematical techniques is important. Recently, qualitative results for physical, chemical and biological systems have been studied extensively [52-54, etc.], and some powerful mathematical methods, such as the Lie symmetry [55-57, etc.], have been developed and widely applied to many nonlinear systems. The goal of this paper is to establish the global structure for the Duffing equation in the Poincaré phase plane under given parametric conditions. From this global structure, some qualitative behaviors of exact solutions of equation (1.1) can be derived directly. Traveling wave solutions of the Klein-Gordon equation (1.2) are accordingly obtained by using exact solutions of equation (1.1).

The organization of this paper is as follows. In Section 2, using the qualitative theory of dynamical systems, we present qualitative analysis of a two-dimensional plane autonomous system which is equivalent to the damped Duffing equation (1.1). In Section 3, we first re-derive an exact solution to Duffing equation (1.1) by applying the Lie symmetry, then we show that the same result can actually be obtained more economically by using the coordinate transformation method [58]. Applications of this approach to the study of traveling wave solutions of equation (1.2) are illustrated. Section 4 is a brief conclusion.

2 Global Structure

Equation (1.1) is equivalent to the two-dimensional autonomous system

$$\begin{cases} \dot{x} = A(x,\ y) = y \\ \dot{y} = B(x,\ y) = -\delta y + \mu x - x^3. \end{cases} \tag{2.1}$$

It is well known that $x = 0$ is a nonhyperbolic fixed equilibrium point of system (2.1) at $\mu = 0$ and the bifurcation diagram of equation (1.1) is a supercritical pitchfork bifurcation with a bifurcation point $(x_0,\ \mu_0) = (0,\ 0)$ (see Figure 2.1). Figure 2.1 also illustrates the attracting domains of the three equilibrium solutions.

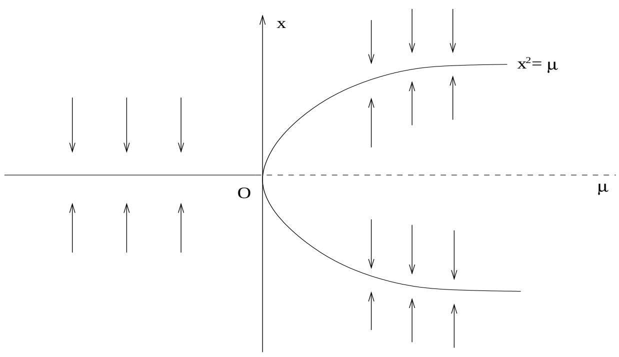

Figure 2.1: Supercritical pitchfork bifurcation.

Note that (2.1) is a two-dimensional plane autonomous system, and $A(x,\ y)$, $B(x,\ y)$ satisfy the conditions of the existence and uniqueness theorem. Throughout this section, we only consider the case where μ is positive in the Poincaré phase plane. (When μ is negative, system (2.1) only has a unique regular equilibrium points (0, 0) and the arguments will be closely similar and relatively less complicated.) There are three regular equilibrium points for system (2.1), namely

$$P(-\sqrt{\mu},\ 0),\quad O(0,\ 0)\ \text{ and }\ R(\sqrt{\mu},\ 0).$$

The corresponding matrix of the linearization of system (2.1) is

$$\begin{bmatrix} 0 & 1 \\ \mu - 3x^2 & -\delta \end{bmatrix}. \tag{2.2}$$

Eigenvalues of (2.2) at O are $-\frac{\delta}{2} \pm \frac{\sqrt{\delta^2+4\mu}}{2}$, so O is a saddle point. Eigenvalues of (2.2) at P and R are $-\frac{\delta}{2} \pm \frac{\sqrt{\delta^2-8\mu}}{2}$. This implies that both P and R are

(i) stable spiral points when $\delta^2 < 8\mu$ and $\delta > 0$;
(ii) unstable spiral points when $\delta^2 < 8\mu$ and $\delta < 0$;
(iii) stable nodes when $\delta^2 \geq 8\mu$ and $\delta > 0$;
(iv) unstable nodes when $\delta^2 \geq 8\mu$ and $\delta < 0$.

A sketch of the phase diagram in the $(x,\ y)$-plane and of the possible profiles of the solutions are shown in Figure 2.2. In the left phase diagram, each orbit corresponds to a typical profile of the bounded solution of equation (1.1). The solution of equation (1.1) associated with the homoclinic orbit A, represents a bell-profile solitary wave. The solution associated with the orbit B exhibits an oscillatory shock wave, and the solution corresponding to the orbit C exhibits a monotone shock wave.

Now, we make the Poincaré transformation as

$$x = \frac{1}{z}, \qquad y = \frac{u}{z}, \qquad d\tau = \frac{dt}{z^2}, \qquad (z \neq 0), \tag{2.3}$$

then (2.1) becomes

$$\begin{cases} \frac{du}{d\tau} = \mu z^2 - 1 - \delta u z^2 - z^2 u^2, \\ \frac{dz}{d\tau} = -u z^3. \end{cases} \tag{2.4}$$

This indicates that there is no equilibrium point on the u-axis for system (2.4). Indeed, one can see that the u-axis is an orbit of system (2.4). On the other hand, through the Poincaré transformation

$$x = \frac{v}{z}, \qquad y = \frac{1}{z}, \qquad d\tau = \frac{dt}{z^2}, \qquad (z \neq 0), \tag{2.5}$$

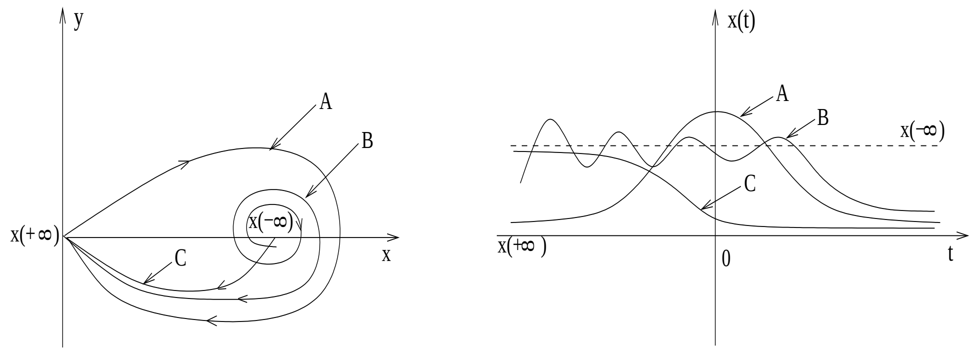

Figure 2.2: The left figure: phase diagram in the (x, y)-plane. The right figure: sketch of typical wave profiles of the solutions of equation (1.1).

(2.1) becomes

$$\begin{cases} \frac{dz}{d\tau} = P(z,\ v) = \delta z^3 - \mu v z^3 + v^3 z, \\ \frac{dv}{d\tau} = Q(z,\ v) = z^2 + \delta v z^2 - \mu v^2 z^2 + v^4. \end{cases} \tag{2.6}$$

Note that the origin is the unique equilibrium point of (2.6) on the v-axis. This implies that system (2.1) has two infinite equilibrium points E and F on the y-axis.

Equation (2.6) is a higher-order two-dimensional autonomous system, since the matrix of corresponding linearization at (0, 0) is

$$\left[\begin{array}{cc} P_v(z,v) & P_z(z,v) \\ Q_v(z,v) & Q_z(z,v) \end{array} \right] \Bigg|_{(z,\ v)=(0,\ 0)} = \left[\begin{array}{cc} 0 & 0 \\ 0 & 0 \end{array} \right].$$

We call the origin, the high-order equilibrium point. To analyze the local structure at the origin, we utilize the polar coordinates to investigate (2.6). In polar coordinate $r = \sqrt{v^2 + z^2}$, $\theta = \arctan(\frac{z}{v})$ with inverse transformation $z = r\cos\theta,\ v = r\sin\theta$, system (2.6) becomes

$$\begin{cases} \dot{r} = r^2[R(\theta) + o(1)] \\ \dot{\theta} = r[D(\theta) + o(1)], \end{cases} \tag{2.7}$$

where $R(\theta) = \sin\theta \cdot \cos^2\theta$ and $D(\theta) = \cos^3\theta$. Solving $D(\theta) = 0$ for θ when $0 \le \theta < 2\pi$, we have

$$\theta_k = \frac{\pi}{2} \text{ and } \frac{3\pi}{2} \quad (k = 1,\ 2).$$

We need the following lemma.

Lemma 2.1: Suppose that T is a trajectory of (2.7) which approaches the equilibrium point (0, 0) along the ray $\theta = \theta_0$ as $t \to +\infty$ or $-\infty$, i.e., the slope of the tangent line of the trajectory T approaches $\tan \theta_0$ as $r \to 0$. Then

$$D(\theta_0) = 0. \tag{2.8}$$

Proof. Assume that $A(r,\ \theta)$ is an arbitrary point on T, and L is a ray passing through the origin and $A(r,\ \theta)$. We know that $\theta \to \theta_0$ as $r \to 0$. Denote α the angle between the line L and the tangent line of the trajectory T at $A(r,\ \theta)$ (see Figure 2.3). Then we have

$$\tan \alpha = \lim_{\Delta r \to 0} r \frac{\Delta \theta}{\Delta r} = r \frac{d\theta}{dr}.$$

Using (2.7), we get

$$\tan \alpha = \frac{D(\theta) + o(1)}{R(\theta) + o(1)}. \tag{2.9}$$

Since $\theta \to \theta_0$ implies $\alpha \to 0$ as $r \to 0$, from (2.9), we obtain (2.8) immediately. $\square$

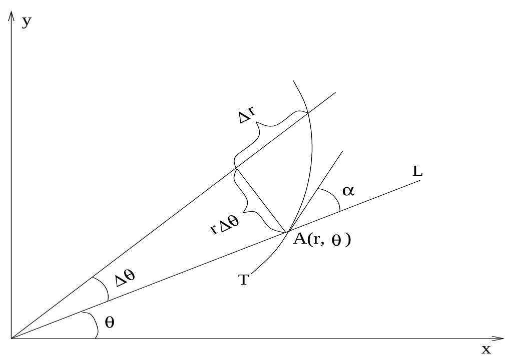

Figure 2.3: Trajectory T.

By virtue of the above Lemma, we know that if system (2.7) has orbits which approach the origin at a definite direction θ as $t \to +\infty$ or $-\infty$, then θ must be equal to one of the $\theta_k' s$ (k=1, 2).

Let ε and r_0 be sufficiently small and construct sectors $u_k = \triangle O\widehat{A_k B_k} = \{(r,\ \theta)\big| r \leq r_0,\ |\theta - \theta_k| \leq \varepsilon\}$ $(k = 1,\ 2)$, (see unshaded sectors in Figure 2.4). Except in these two $u_k's$, $D(\theta)$ has the same sign for all points in each shaded sector. One can see that in each shaded sector, θ which can be considered as a function of the time alone, is monotone with respect to t. That is, each orbit inside a shaded sector must travel from one side (OA_k or OB_k) to the other side (OB_k or OA_k). No orbit can approach the origin O inside shaded sectors as $t \to +\infty$ or $-\infty$, this is because we assume that $D(\theta) \neq 0$ in a shaded sector denoted by $\triangle O\widehat{A_l B_m}$ $(l = 1,\ m = 2$, or $l = 2,\ m = 1)$. Denote $\bar{\theta_1}$ the angle between the segment line OA_l and OB_m. Then

$$\min_{0 \leq \theta \leq \bar{\theta_1}} \big|D(\theta)\big| = c > 0.$$

Let r_1 be sufficiently small such that in the shaded sector $\triangle O\widehat{A_l B_m}$ (see Figure 2.4) we have

$$\big|D(\theta) + o(1.1)\big| > \frac{c}{2} > 0,$$

and

$$\sup_{(r,\ \theta) \in \triangle O\widehat{A_l B_m}} \Big|\frac{R(\theta) + o(1)}{D(\theta) + o(1)}\Big| = M < +\infty. \tag{2.10}$$

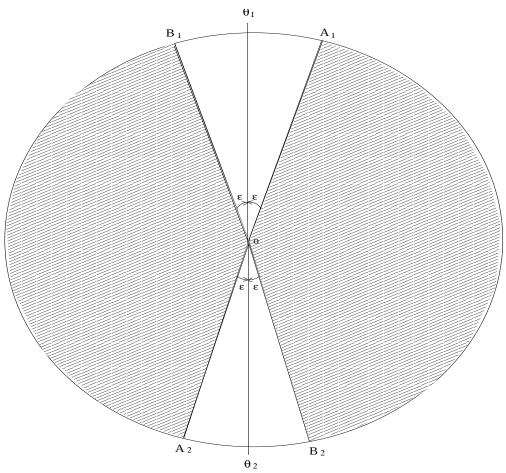

Figure 2.4: Sectors OA_kB_k (k=1, 2).

From the second equation of (2.7), we obtain $\dot{\theta} \neq 0$ whenever θ is inside $\triangle O\widehat{A_l B_m}$. Namely, θ is monotone increasing with respect to t when $D(\theta) > 0$ and monotone decreasing when $D(\theta) < 0$.

Suppose that $r(\theta)$ is an arbitrary orbit emanating from $(\bar{\theta}_0,\ r(\bar{\theta}_0))$, where $0 < \bar{\theta}_0 < \bar{\theta}_1$ and $0 < r(\bar{\theta}_0) < r_0$. Let $\bar{\theta}_2$ satisfy $0 < |\bar{\theta}_2 - \bar{\theta}_0| \leq \bar{\theta}_1$ and such that the whole part of the orbit associated with $[\bar{\theta}_0,\ \bar{\theta}_2]$ is inside $\triangle O\widehat{A_l B_m}$. Then

$$\frac{1}{r}\frac{dr}{d\theta} = \frac{R(\theta) + o(1)}{D(\theta) + o(1)}, \quad r \to 0. \tag{2.11}$$

Integrating (2.11) from $\bar{\theta}_0$ to θ ($\bar{\theta}_0 \leq \theta < \bar{\theta}_1$), then yields

$$\int_{r(\bar{\theta}_0)}^{r(\theta)} \frac{dr}{r} = \int_{\bar{\theta}_0}^{\theta} \frac{R(\theta) + o(1)}{D(\theta) + o(1)} d\theta. \tag{2.12}$$

From (2.10) and (2.12), we have

$$\left| \ln \frac{r(\theta)}{r(\bar{\theta}_0)} \right| \leq M|\theta - \bar{\theta}_0| < M(\bar{\theta}_1 - \bar{\theta}_0) < +\infty. \tag{2.13}$$

Formula (2.13) implies that when $r(\bar{\theta}_0) > 0$, $r(\theta)$ must be positive inside $\triangle O\widehat{A_l B_m}$. In the case where $r(\bar{\theta}_0)$ gets smaller and smaller, $r(\theta)$ must become smaller and smaller simultaneously. However, no matter how smaller $r(\bar{\theta}_0)$ be changed to, $r(\theta)$ can not be equal to zero. Otherwise, the expression on the left hand side of (2.13) will be unbounded. This indicates that no orbit can approach the origin as the time increases or decreases.

Based on Lemma 2.1 and the above analysis, we can now obtain the following Theorem 2.1 and use it to determine the global structure of system (2.1).

Theorem 2.1: Suppose that θ_k ($k = 1,\ 2$) are zero points of $D(\theta)$ and

$$\begin{aligned} &D^{(i)}(\theta_k) = 0, \quad 0 \leq i \leq p-1, \quad D_p = D^{(p)}(\theta_k) \neq 0, \\ &R^{(i)}(\theta_k) = 0, \quad 0 \leq i \leq q-1, \quad R_q = D^{(q)}(\theta_k) \neq 0, \end{aligned} \tag{2.14}$$

where q is even and $p > q$, Then

(a) If $p-q$ is odd, D_p and R_q have the same sign in the sector $\triangle O\widehat{A_k B_k}$, then all orbits of (2.7) inside $\triangle O\widehat{A_k B_k}$ approach the origin in the direction of $\theta = \theta_k$ as $t \to +\infty$ or $-\infty$.

(b) If $p - q$ is odd, D_p and R_q have different signs in the region $\triangle O\widehat{A_k B_k}$, then there exists at least one orbit of (2.7) inside $\triangle O\widehat{A_k B_k}$ which approaches the origin in the direction of $\theta = \theta_k$ as $t \to +\infty$ or $-\infty$, respectively.

(c) If $p-q$ is even, there are two possibilities. Either there is no orbit of (2.7) inside $\triangle O\widehat{A_k B_k}$ which approaches the origin as $t \to +\infty$ or $-\infty$, or there are infinitely many orbits of (2.7) inside $\triangle O\widehat{A_k B_k}$ which approach the origin in the direction of $\theta = \theta_k$ as $t \to +\infty$ or $-\infty$.

Proof. (a) Using the conditions (2.14) and the Taylor's series, when θ gets close to θ_k, $D(\theta)$ and $\tan\alpha$ can be expressed as follows

$$\begin{aligned} \tan\alpha &= \frac{D_p}{R_q} \cdot (\theta - \theta_k)^{p-q} + o(|\theta - \theta_k|^{p-q}) + o(1), \quad \text{as} \quad r \to 0, \\ D(\theta) &= \frac{D^{(p)}(\theta_k)}{p!}(\theta - \theta_k)^p + o(|\theta - \theta_k|^p). \end{aligned} \tag{2.15}$$

When $p-q$ is odd and $\frac{D_p}{R_q} > 0$, one can see that $\tan\alpha < 0$ on OA_k and $\tan\alpha > 0$ on OB_k.

Let ε be sufficiently small such that $R(\theta)$ and R_q have the same sign inside $\triangle O\widehat{A_k B_k}$. Also, let r_0 be sufficiently small such that $R(\theta) + o(1)$ and $R(\theta)$ have the same sign, and

$$\big|R(\theta) + o(1.1)\big| > \frac{|R_q|}{2} > 0. \tag{2.16}$$

First, we assume that $R_q < 0$ and $D^{(p)}(\theta_k) < 0$. From (2.16), inside $\triangle O\widehat{A_k B_k}$, we have

$$R(\theta) + o(1) < \frac{R_q}{2} < 0.$$

Since $\dot{r} = r^2[R(\theta) + o(1)]$, this implies that inside the sector $\triangle O\widehat{A_k B_k}$, from each point except the origin O, we have $\dot{r} < 0$. Thus, on the boundary of the sector $\triangle O\widehat{A_k B_k}$, all orbits at each point point inward (see Figure 2.5, left graph, where the direction of the arrow represents the direction of each orbit when t increases). In other words, the sector $\triangle O\overset{\frown}{A_kB_k}$ is a positive invariant domain for all orbits, and for each point on the orbit inside $\triangle O\overset{\frown}{A_kB_k}$, r is decreasing as the time t increases.

For two arbitrary numbers r_1 and r_2, if $0 < r_2 < r_1 < r_0$, the time for the orbit traveling from r_1 to r_2 is

$$\begin{aligned} t_2 - t_1 &= \int_{r_1}^{r_2} \frac{dr}{r^2[R(\theta) + o(1)]} \\ &\le \int_{r_2}^{r_1} \frac{dr}{r^2 \frac{|R_q|}{2}} \\ &= \frac{2}{3|R_q|}\Big(\frac{1}{r_2^3} - \frac{1}{r_1^3}\Big). \end{aligned}$$

This means that all orbits inside the sector $\triangle O\overset{\frown}{A_kB_k}$ will enter a neighborhood of the origin O, no matter how small this neighborhood is as t increases. Thus, they will approach the origin as $t \to +\infty$. Recall our previous assumption that ε is sufficiently small. Applying the Lemma, we can conclude that all orbits of (2.7) inside the sector $\triangle O\overset{\frown}{A_kB_k}$ go to the origin O in the direction $\theta = \theta_k$ as $t \to +\infty$.

For the case $R_q > 0$ and $D_p > 0$, making a transformation $t \to -t$ and using the same discussion, we obtain that all orbits of (2.7) inside the sector $\triangle O\overset{\frown}{A_kB_k}$ go to the origin O in the direction $\theta = \theta_k$ as $t \to -\infty$.

(b) Consider the case $R_q < 0$ and $D_p > 0$ first. Using almost the same arguments as in case (a), we can obtain that all orbits at each point on the sides OA_k and OB_k point outward, but at each point on the arc $\overset{\frown}{A_kB_k}$, the orbits point inward. Suppose that M is a point on OA_k and the orbit L_1 passes through M. As t decreases, L_1 must intersect $\overset{\frown}{A_kB_k}$ at some point, denoted by P_M. If M goes to the origin O, then P_M will approach some point denoted by P_1, where $P_1 \in \overset{\frown}{A_kB_k}$. On the other hand, suppose that N is a point on OB_k and the orbit L_2 passes through N. As t decreases, L_2 must intersect $\overset{\frown}{A_kB_k}$ at some point, denoted by P_N. If N goes to the origin O, then P_N will approach some point denoted by P_2, where $P_2 \in \overset{\frown}{A_kB_k}$. There are only two possibilities here. If P_1 coincides with P_2, then we can conclude that there is a unique orbit which approaches the origin O as t goes to $+\infty$. If P_1 is different from P_2, each orbit which passes through the points between $\overset{\frown}{P_1P_2}$ will approach the origin O as $t \to +\infty$.

For the case $R_q > 0$ and $D_p < 0$, one can proceed in the same manner, and obtain that there exists at least one orbit of (2.7) inside $\triangle O\overset{\frown}{A_kB_k}$ which approaches the origin in the direction of $\theta = \theta_k$ as $t \to -\infty$.

(c) Consider $R_q < 0$ first. If $D_p < 0$, using (2.15) and the same arguments as shown in part (a), each orbit of (2.7) on OA_k points outward and each orbit of (2.7) on OB_k or the arc $\overset{\frown}{A_kB_k}$ points inward (see Figure 2.5, right graph).

Figure 2.5: Local structures in the $(x,\ y)$ plane of cases (a) and (c).

Suppose that M_0 is a point on OA_k and l_1 is an orbit of (2.7) passing through M_0. Then l_1 must intersect the arc $\overset{\frown}{A_kB_k}$ or the segment line OB_k at some point P_3 as t decreases. When M_0 moves closer and closer to the origin O, P_3 must get closer and closer to some point P_0 on the arc $\overset{\frown}{A_kB_k}$ or the segment line OB_k. If P_0 is the origin O, then there is no orbit inside the sector $\triangle O\overset{\frown}{A_kB_k}$ to approach the origin as $t \to +\infty$ or $-\infty$. If P_0 does not coincide with the origin O, then any orbit of (2.7) departing from the point which lies on $OB_k \cup \overset{\frown}{B_kP_0}$ (when $P_0 \in \overset{\frown}{A_kB_k}$) or OP_0 (when $P_0 \in OB_k$) will approach the origin O as $t \to +\infty$ or $-\infty$. The arguments for the case of $D^{(p)}(\theta_k) > 0$ are almost the same as the above. So we omit the details.

For the case $R_q > 0$, the discussions are closely similar to those of the case $R_q < 0$ by making the transformation $t \to -t$. The corresponding graphs can be obtained by reversing the directions of arrows.

□

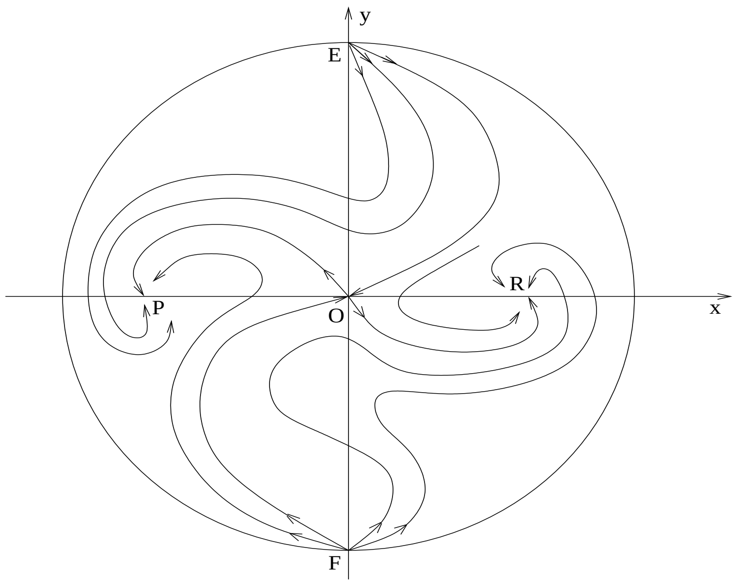

Figure 2.6: Global structure in the $(x,\ y)$ plane when $\delta > 0$ and $\delta^2 \geq 8\mu$.

For now, we limit our attention to the unshaded sectors $\triangle O\widehat{A_k B_k}$ $(k = 1,\ 2)$, and divide our arguments into two parts as follows:

(i) In the case $\theta_1 = \frac{\pi}{2}$, we have

$$D(\theta_1) = 0, \quad R(\theta_1) = 0$$

and

$$\begin{aligned}
D'(\theta_1) &= -3\sin\theta_1\cos^2\theta_1\big|_{\theta_1=\pi/2} = 0, \\
D''(\theta_1) &= 6\cos\theta_1\sin^2\theta_1 - 3\cos^3\theta_1\big|_{\theta_1=\pi/2} = 0, \\
D'''(\theta_1) &= -6\sin^3\theta_1 + 12\sin\theta_1\cos^2\theta_1 + 9\cos\theta_1\sin\theta_1\big|_{\theta_1=\pi/2} = -6, \\
R'(\theta_1) &= \cos^3\theta_1 - 2\sin^2\theta_1\cos\theta_1\big|_{\theta_1=\pi/2} = 0, \\
R''(\theta_1) &= -3\cos^2\theta_1\sin\theta_1 + 2\sin^3\theta_1 - 4\cos^2\theta_1\sin\theta_1\big|_{\theta_1=\pi/2} = 2.
\end{aligned}$$

When θ is close to θ_1, using the Taylor expansion, we have

$$\begin{aligned} D(\theta) &= \frac{D'''(\theta_1)}{3!}(\theta-\theta_1)^3 + o(|\theta-\theta_1|^3) \\ &= -(\theta-\theta_1)^3 + o(|\theta-\theta_1|^3), \\ R(\theta) &= \frac{R''(\theta_1)}{2!}(\theta-\theta_1)^2 + o(|\theta-\theta_1|^2) \\ &= (\theta-\theta_1)^2 + o(|\theta-\theta_1|^2). \end{aligned}$$

Thus, we get

$$\tan\alpha = r\frac{d\theta}{dr} = \frac{D'''(\theta_1)}{3R''(\theta_1)} \cdot (\theta-\theta_1) + o(|\theta-\theta_1|) + o(1), \quad r \to 0, \tag{2.17}$$

where α is described as in Figure 2.3.

(ii) In the case $\theta_2 = \frac{3\pi}{2}$, similarly we have

$$\begin{aligned} &D(\theta_2) = 0, \quad R(\theta_2) = 0, \\ &D'(\theta_2) = 0, \quad D''(\theta_2) = 0, \\ &D'''(\theta_2) = 6, \quad R'(\theta_2) = 0, \\ &R''(\theta_2) = -2. \end{aligned}$$

and

$$\tan\alpha = r\frac{d\theta}{dr} = -(\theta-\theta_2) + o(|\theta-\theta_2|) + o(1), \quad r \to 0, \tag{2.18}$$

where α is described as in Figure 2.3.

Since the leading coefficients in (2.17) and (2.18) are negative, combining Lemma 2.1 and Theorem 2.1, we are ready to plot the global structure of system (2.1) as Figure 2.6 for parametric choices $\delta^2 \geq 8\mu$ and $\delta > 0$. Here it is worth noting that the points E and F represent the equilibria at infinity. The Poincaré transformation $d\tau = \frac{dt}{z^m}$ used in (2.3) and (2.5) tells us that the local structure of E is the same as that of F when the natural number m is even. When m is odd, the local structure of E is exactly opposite to that of F. That is, the direction of each orbit near E is reversed as the one near F.

The global structure of system (2.1) provides us useful information about the exact solution of the damped Duffing equation (1.1). First, since $\frac{\partial A(x,\ y)}{\partial x} + \frac{\partial B(x,\ y)}{\partial y} = -\delta$, by the Bendixson Theorem, Figure 2.6 has neither closed orbit nor heteroclinic orbit. This means that equation (1.1) has neither bell-profile solitary wave solutions nor nontrivial periodic solutions. Second, we observe that except the equilibrium points $P,\ O,\ R$ and the orbits $L(O,\ P)$ (or $L(P,\ O)$) and $L(O,\ R)$ (or $L(R,\ O)$) , all other orbits in the global structure either emanate from the infinite equilibria E and F or terminate at E and F. This means that the y-coordinate of the point which lies on all those orbits must be unbounded. Consequently the corresponding x-coordinate of the point must be unbounded, too. Otherwise, there exists a positive number ρ such that $|x| < \rho$ as $y \to \infty$. By the Mean-value Theorem, $\frac{dy}{dx}$ is unbounded. Nevertheless, we know that the slope of the tangent lines to those orbits at the point $(x,\ y)$ is given by

$$\frac{dy}{dx} = -\delta + \frac{\mu x - x^3}{y},$$

which indicates that $\frac{dy}{dx}$ is bounded. This is a contradiction. Third, we observe that under the parametric conditions $\delta^2 \geq 8\mu$ and $\delta > 0$, the damped Duffing equation (1.1) only has two nontrivial bounded exact solutions which correspond to the orbits $L(O,\ P)$ and $L(O,\ R)$, respectively. These two solutions represent monotone shock waves. As t goes to positive or negative infinity, each of them tends to a constant.

3 Exact Solutions and Applications

In this section, we will restrict our attention to exact solutions of the Duffing equation (1.1) and their applications to traveling wave solutions of the 2D dissipative Klein-Gordon equation (1.2). We are going to show that an analytic result obtained by the Lie symmetry method can be derived more effectively by means of the coordinate transformation method.

If we use the Lie symmetry to study system (2.1), first we need to look for invariance of (2.1) under a one-parameter infinitesimal point transformations of the form

$$\begin{aligned} &X_i = x_i + \epsilon\eta_i(t,\ x_i) \quad i = 1,\ 2, \\ &T = t + \epsilon\xi(t,\ x_i). \end{aligned}$$

The corresponding infinitesimal generator is

$$V = \xi(t,\ x_i)\frac{\partial}{\partial t} + \eta(t,\ x_i)\frac{\partial}{\partial t}. \tag{3.1}$$

Following [33], in order to find the first prolongation of the vector V, we take $\xi = 0$ in (3.1) and define the associated first extended operator

$$Pr^{(1)}V = \eta_i\frac{\partial}{\partial x_i} + \dot{\eta}_i\frac{\partial}{\partial \dot{x}_i},$$

where $\dot{\eta}_i = D_t\eta_i,\ i = 1,\ 2$ and D_t is the total differential operator. V is called the generator of a one-parameter symmetry group for (2.1) if, whenever (2.1) is satisfied and the following holds:

$$Pr^{(1)}V(\triangle_i)|_{(3)} = \Big(\eta_i\frac{\partial}{\partial x_i} + \dot{\eta}_i\frac{\partial}{\partial \dot{x}_i}\Big)(\triangle_i) = 0, \tag{3.2}$$

where the $\triangle_i's$ $(i = 1,\ 2)$ denote two equations in (2.1). In order to identify a nontrivial infinite dimensional Lie algebra of symmetry vector fields which can be directly associated with the integral of motion for a suitable parametric choice, Senthil and Lakshmanan [33] assumed that the the Lie symmetries η_i $(i = 1,\ 2)$ in (3.2) have the cubic form

$$\begin{aligned} \eta_1 &= a_1 + a_2y + a_3y^2 + a_4y^3, \\ \eta_2 &= b_1 + b_2y + b_3y^2 + b_4y^3, \end{aligned} \tag{3.3}$$

where the $a_i's$ and $b_i's$ $(i = 1,\ 2,\ 3,\ 4)$ are functions of t and x. Substituting (3.3) into (3.2) and equating the coefficients of various powers of y, one can get the resultant determining equations

$$\begin{aligned}
&a_{4x} = b_{4x} = 0, \\
&a_{4t} + a_{3x} - 3\delta a_4 - b_4 = 0, \\
&b_{4t} + b_{3x} - 2\delta b4 + (3x^2 - \mu)a_4 = 0, \\
&a_{3t} + a_{2x} - 2\delta a_3 - 3(x^3 - \mu)a_4 - b_3 = 0, \\
&b_{3t} + b_{2x} - 3(x^3 - \mu x)b_4 - \delta b_3 + (3x^2 - \mu)a_3 = 0, \\
&a_{2t} + a_{1x} - \delta a_2 - 2(x^3 - \mu x)a_3 - b_2 = 0, \\
&b_{2t} + b_{1x} - 2(x^3 - \mu x)b_3 + (3x^2 - \mu)a_2 = 0, \\
&a_{1t} - a_2(x^3 - \mu x) - b_1 = 0, \\
&b_{1t} - b_2(x^3 - \mu x) + c_1b_1 + a_1(3x^2 - \mu) = 0.
\end{aligned}$$

When

$$2\delta^2 = -9\mu, \tag{3.4}$$

with the aid of Maple software, the above determining equations can be solved and four vector fields are obtained as follows

$$\begin{aligned}
S_1 &= X = y\frac{\partial}{\partial x} - (\delta y + x^3 + \frac{2}{9}\delta^2 x)\frac{\partial}{\partial y},\\
S_2 &= e^{(1/3)\delta t}[(y + \frac{1}{3}\delta x)\frac{\partial}{\partial x} - (\frac{1}{3}\delta y + x^3 + \frac{1}{9}\delta^2 x)\frac{\partial}{\partial x}],\\
S_3 &= e^{(4/3)\delta t}(y^2 + \frac{2}{3}\delta xy + \frac{1}{2}x^4 + \frac{1}{9}\delta^2 x^2)S_1,\\
S_4 &= e^{(4/3)\delta t}(y^2 + \frac{2}{3}\delta xy + \frac{1}{2}x^4 + \frac{1}{9}\delta^2 x^2)S_2,
\end{aligned}$$

where X is the dynamical vector field. Since the vector fields S_3 and S_4 are not functionally independent, one can use them to generate the integral of motion M associated with the dynamical system (2.1) as follows

$$M = \exp\big(\frac{4}{3}\delta t\big)\big(y^2 + \frac{2}{3}\delta xy + \frac{1}{2}x^4 + \frac{1}{9}\delta^2 x^2\big). \tag{3.5}$$

Combining (3.5) and (2.1), one can thus find the exact solution to Duffing's equation (1.1)

$$x(t) = (\sqrt{2}\delta/3)c_0 e^{(-\delta t/3)}\mathrm{cn}(c_0 v;\ k), \quad v = -\sqrt{2}e^{(-\delta t/3)} - c_1 \tag{3.6}$$

where c_0 and c_1 are arbitrary integration constants and $k^2 = \frac{1}{2}$. It is notable that for exactly the same parametric choice (3.4), the exact solution (3.6) can be obtained by using the elliptic function method [32] and the Painlevé analysis [31] independently.

Here, we wish to point out that the above exact solution (3.6) and traveling wave solutions to some nonlinear evolution equations, such as the 2D dissipative Klein-Gordon equation (1.2) and the non-integrable Newell-Whitehead equation [59]

$$u_t - u_{xx} = \alpha u - \beta u^3$$

can be obtained more effectively by utilizing the coordinate transformation method. Now, we merely use the 2D dissipative Klein-Gordon equation (1.2) as an example. Assume that the Klein-Gordon equation (1.2) has a traveling wave solution of the form

$$u(x,\ y,\ t) = u(\xi), \quad \xi = kx + ly - \lambda t, \tag{3.7}$$

where k, l and λ are real constants. Substituting (3.7) into (1.2) gives

$$u_{\xi\xi} - \frac{\alpha\lambda}{\lambda^2 - k^2 - l^2} u_\xi + \frac{\beta}{\lambda^2 - k^2 - l^2} u + \frac{\gamma}{\lambda^2 - k^2 - l^2} u^3 = 0. \tag{3.8}$$

Note that the coefficient of u^3 can be changed to 1 by rescaling (3.8) with $u = \eta u$, thus, it reduces to the damped Duffing equation (1.1) and the previous discussions on the damped Duffing equation apply. But this is not necessary in view of our arguments below.

Following [58], we make the natural logarithmic transformation

$$\xi = \frac{\lambda^2 - k^2 - l^2}{\alpha\lambda} \ln \tau.$$

Then equation (3.8) becomes

$$\frac{\alpha^2\lambda^2}{(\lambda^2 - k^2 - l^2)^2} \tau^2 \frac{d^2 u}{d\tau^2} + \frac{\beta}{\lambda^2 - k^2 - l^2} u + \frac{\gamma}{\lambda^2 - k^2 - l^2} u^3 = 0. \tag{3.9}$$

Next, take the nonlinear transformation as

$$q = \tau^k, \quad u = \tau^{-\frac{1}{2}(k-1)} \cdot P(q),$$

then equation (3.9) becomes

$$\frac{d^2 P}{dq^2} = -\frac{\gamma(\lambda^2 - k^2 - l^2)}{\alpha^2\lambda^2 k^2} q^{\frac{1-3k}{k}} P^3(q), \tag{3.10}$$

where $k^2 = 1 - \frac{4\beta(\lambda^2 - k^2 - l^2)}{\alpha^2\lambda^2}$.

Letting $k = \frac{1}{3}$, we get

$$2\alpha^2\lambda^2 = 9\beta(\lambda^2 - k^2 - l^2),$$

and equation (3.10) reduces to

$$p''(w) = -\frac{9\gamma(\lambda^2 - k^2 - l^2)}{\alpha^2\lambda^2} p^3(w). \tag{3.11}$$

Since equation (3.11) has a particular solution

$$p(w) = \pm\frac{\sqrt{2}}{3} \frac{\alpha\lambda}{\sqrt{\gamma(k^2 + l^2 - \lambda^2)}} \frac{1}{w + c},$$

where c is arbitrary constant, the Klein-Gordon has traveling wave solutions

$$u_1(x,\ y,\ t) = \pm\frac{\sqrt{2}}{3}\frac{\alpha\lambda}{\sqrt{\gamma(k^2+l^2-\lambda^2)}}\frac{\exp\left[\frac{\alpha\lambda}{3(\lambda^2-k^2-l^2)}(kx+ly-\lambda t+\xi_0)\right]}{\exp\left[\frac{\alpha\lambda}{3(\lambda^2-k^2-l^2)}(kx+ly-\lambda t+\xi_0)\right]+c_0}, \tag{3.12}$$

where both ξ_0 and c_0 are arbitrary constants. From (3.12), one can see that when c_0 is positive, u_1 describes a kink-profile traveling wave which is actually monotone with respect to ξ. It is analytic for all $(x,\ y,\ t)$, but blows up at infinite points of $(x,\ y,\ t)$ when c_0 is negative.

Equation (3.11) can be converted to the canonical form of an elliptical integral of the first kind after multiplying (3.11) by p' and performing one integration:

$$[p'(w)]^2 = \frac{9\gamma(k^2+l^2-\lambda^2)}{2\alpha^2\lambda^2}p^4(w) + c_2.$$

where c_2 is arbitrary constant. Choosing $c_2 = 1$ or -1, respectively, and changing to the original variables, we obtain that the Klein-Gordon equation has traveling wave solutions

$$\begin{aligned} u_2(x,\ y,\ t) &= \pm\sqrt{\frac{2\alpha^2\lambda^2}{9\gamma(k^2+l^2-\lambda^2)}}\exp\left(\frac{\alpha\lambda}{3(\lambda^2-k^2-l^2)}(kx+ly-\lambda t+\xi_0)\right) \\ &\quad \cdot\mathrm{nc}\Big\{\pm\sqrt{2}\Big[\exp\left(\frac{\alpha\lambda}{3(\lambda^2-k^2-l^2)}(kx+ly-\lambda t+\xi_0)\right)+c_3\Big];\frac{1}{\sqrt{2}}\Big\}, \end{aligned} \tag{3.13}$$

$$\begin{aligned} u_3(x,\ y,\ t) &= \pm\sqrt{\frac{2\alpha^2\lambda^2}{9\gamma(\lambda^2-k^2-l^2)}}\exp\left(\frac{\alpha\lambda}{3(\lambda^2-k^2-l^2)}(kx+ly-\lambda t+\xi_0)\right) \\ &\quad \cdot\mathrm{sd}\Big\{\pm\sqrt{2}\Big[\exp\left(\frac{\alpha\lambda}{3(\lambda^2-k^2-l^2)}(kx+ly-\lambda t+\xi_0)\right)+c_3\Big];\frac{1}{\sqrt{2}}\Big\}, \end{aligned} \tag{3.14}$$

where ξ_0 and c_3 are arbitrary constants.

By comparison with the previous methods described in [31-33, 59], the coordinate transformation method we use here for the damped Duffing equation (3.8) to obtain its exact solutions appears to be more straightforward and involves less calculations. It is notable that the Jacobian elliptic functions nc and sd in (3.13) and (3.14) oscillate more and more strongly as $\frac{\alpha\lambda}{3(\lambda^2-k^2-l^2)}(kx+ly-\lambda t+\xi_0) \to +\infty$. Moreover, the elliptic function in (3.6) has singularities that are more and more closely spaced. At this moment, we are still wondering under what circumstances traveling wave solutions (3.13) and (3.14) have any physical or chemical applications.

4 Conclusion

One of the most fundamental equations in the study of the nonlinear oscillations is the Duffing equation. It has been discussed in many papers arising in various scientific fields. The damped Duffing equation is non-integrable. Although its local behavior has been well studied and understood, the global structure of the damped Duffing equation does not seem to have been carefully studied, to the best of our knowledge. Therefore, qualitative analysis as well as innovative mathematical techniques are in order.

In this paper, under certain parametric conditions, we apply qualitative theory of planar systems to show the global structure of a two-dimensional plane autonomous system, which is equivalent to the damped Duffing equation (1.1). The exact solution to the damped Duffing equation is presented and traveling wave solutions of the 2D dissipative Klein-Gordon equation (1.2) are derived by applying the coordinate transformation method.

Acknowledgment: The work has been presented at the Applied Mathematics Seminar, University of Texas-Pan American, Edinburg, TX, on January 27, 2005.

5 References

[1] Jordan D.W. and Smith P., Nonlinear Ordinary Differential Equations, Clarendon Press, Oxford, 1977.

[2] Thompson J.M.T. and Stewart H.B., Nonlinear Dynamics and Chaos, John Wiley & Sons, New York, 1986.

[3] Pezeshki C. and Dowell E.H., An examination of initial condition maps for the sinusoidally excited buckled beam modeled by the Duffing's equation, J. Sound Vibration, 117 (1987) 219-232.

[4] Moon F.C., Chaotic Vibrations: An Introduction for Applied Scientists and Engineers, John Wiley & Sons, New York, 1987.

[5] Dowell E.H. and Pezeshki C., On the understanding of chaos in Duffing's equation including a comparison with experiment, Trans. ASME J. Appl. Mech. 53 (1986) 5-9.

[6] Ku Y.H. and Sun X.G., Chaos and limit cycle in Duffing's equation, J. Franklin Inst. 327 (1990) 165-195.

[7] Battelli F. and Palmer K.J., Chaos in the Duffing equation, J. Diff. Equs. 101 (1993) 276-301.

[8] Loria A., Panteley E. and Nijmeijer H., Control of the chaotic Duffing equation with uncertainty in all parameters, IEEE Trans. Circuits Syst. I 45 (1998) 1252-1255.

[9] Chen G. and Dong X., From Chaos to Order: Perspetives, Methodologies and Applications, World Scientific Press, Singapore, 1998.

[10] Jiang Z.P., Advanced feedback control of the chaotic Duffing's equation, IEEE Trans. Circuits Syst. I 49 (2002) 244-249.

[11] Nijmeijer H. and Berghuis H., On Lyapunov control of the Duffing equation, IEEE Trans. Circuits Syst. I 42 (1995) 473-477.

[12] Holmes P.J., A nonlinear oscillator with a strange attractor, Proc. R. Sot. 292 (1979) 419-448.

[13] Moon F.C. and Holmes P.J., A magnetoelastic strange attractor, J. Sound Vibrations, 65 (1979) 275-296.

[14 Holmes P.J. and Moon F.C., Strange attractors and chaos in nonlinear mechanics, J. Appl. Mech. 50 (1983) 1021-1032.

[15] Seydel R., Attractors of a Duffing equation-dependence on the exciting frequency, Phys. D 17 (1985) 308-312.

[16] Holmes P. and Whitley D., On the attracting set for Duffing's equation, Phys. D 7 (1983) 111-123.

[17] McCartin B.J., An alternative analysis of Duffing's equation, SIAM Rev. 34 (1992) 482-491.

[18] Blair K.B., Krousgrill C.M. and Farris T.N., Harmonic balance and continuation techniques in the dynamic analysis of Duffing's equation, J. Sound Vibration, 202 (1997) 717-731.

[19] Holmes P.J., New Approaches to Nonlinear Problems in Dynamics, SIAM, Philadelphia, PA, 1981.

[20] Habets P. and Metzen G., Existence of perodic solutions of Duffing's equation, J. Diff. Equs. 78 (1989) 1-32.

[21] Wang H.Z. and Li Y., Existence and uniqueness of periodic solutions for Duffing equation, J. DifF. Equs. 108 (1994) 152-169.

[22] Wang C.W., Multiplicity of periodic solutions for Duffing equation under nonuniform non-resonance conditions, Proc. Amer. Math. Soc. 126 (1998) 1725-1732.

[23] Ding T.R., Iannacci R. and Zanolin F., On periodic solutions of sublinear Duffing equations, J. Math. Anal. Appl. 158 (1991) 316-332.

[24] Fang T. and Dowell E.H., Numerical simulations of jump phenomena in stable Duffing systems, Internat. J. Non-Linear Mech. 22 (1987) 267-274.

[25] Khuri S.A. and Xie S.S., On the numerical verification of the asymptotic expansion of Duffing's equation. Internat. J. Comput. Math. 72 (1999) 325-330.

[26] Matsuo T. and Kishima A., Numerical analysis of bifurcations in Duffing's equation with hysteretic functions, Electron. Comm. Japan Part III Fund. Electron. Sci. 75 (1992) 61-71.

[27] Murray J.D., Mathematical Biology, Springer-Verlag, New York, 1993.

[28] Zhang Z.F., Ding T.R., Huang W.Z. and Dong Z.X., Qualitative Analysis of Nonlinear Differential Equations, Science Press, Beijing, 1997.

[29] Chen Y.Z., Solutions of the Duffing equation by using target function method, J. Sound Vibration, 256 (2002) 573-578.

[30] Ince E.L., Ordinary Differential Equations, Dover Publications, New York, 1956.

[31] Parthasarathy S. and Lakshmanan M., On the exact solutions of the Duffing oscillator, J. Sound Vibration, 137 (1990) 523-526.

[32] Lawden D.F., Elliptic Functions and Applications, Springer-Verlag, New York, 1989.

[33] Senthil M. and Lakshmanan M., Lie symmetries and infinite-dimensional Lie algebras of certain nonlinear dissipative systems, J. Phys. A (Math. Gen.) 28 (1995) 1929-1942.

[34] Hale J.K. and Spezamiglio A., Perturbation of homoclinics and subharmonics in Duffing's equation, Nonlin. Anal. 9 (1985) 181-192.

[35] Lions J.L., Quelques méthods de résolution des problémes aux limites non linéaires, Dunod/GauthierVillars, Paris, 1969.

[36] Temam R., Infinite-Dimensional Dynamical Systems in Mechanics and Physics (2nd ed.), Vol.68, Springer-Verlag, 1997.

[37] Bjorken J.D. and Drell S.D., Relativistic Quantum Fields, McGraw-Hill Book Co., New York, 1964.

[38] Hobart R.H., On the instability of a class of unitary field models, Proc. Phys. Soc. 82 (1963) 201-203.

[39] Bishop A.R. and Schneider T., Solitons and Condensed Matter Physics, Springer, Berlin, 1978.

[40] Chiao R.Y., Garmire E. and Townes C.H., Geometrical phases from global gauge invariance of nonlinear classical field theories, Phys. Rev. Lett. 13 (1964) 479-482.

[41] Korpel A., Two-dimensional plane wave theory of strong acousto-optic interaction in isotropic media, Proc. IEEE, 67 (1979) 1442-1443.

[42] Banerjee P.P. and Cao G., Periodic and aperiodic solitary wave solutions of the nonlinear Klein-Gordon equation without dispersion, J. Phys. A (Math. Gen.) 21 (1988) 55-71.

[43] Li S. and Vu-Quoc L., Finite difference calculus invariant structure of a class of algorithms for the nonlinear Klein-Gordon equation. SIAM J. Numer. Anal. 32 (1995) 1839-1875.

[44] Ha J.H. and Nakagiri S., Identification problems for the damped Klein-Gordon equation, J. Math. Anal. Appl. 289 (2004) 77-89.

[45] Banks H.T. and Smith R.C., Smart Material Structures: Modeling, Estimation and Control, Masson, Paris, 1996.

[46] Bradley M.E. and Lenhart S., Bilinear spatial control of the velocity term in a Kirchhoff plate equation, Electron. J. Diff. Equs. 27 (2001) 115.

[47] Kosechi R., The unit condition and global existence for a class of nonlinear Klein-Gordon equation, J. Diff. Equs., 100 (1992) 257-268.

[48] Geoggiev V., Decay estimates for the Klein-Gordon equation, Comm. Partial Diff. Equs., 17 (1992) 1111-1139.

[49] Ozawa T., Tsutaya K. and Tsutsumi Y., Global existence and asymptotic behavior of solutions for the Klein-Gordon equations with quadratic nonlinearity in two dimensional space, Math. Z. 222 (1996) 341-362.

[50] Gao P. and Guo B.L., The time-periodic solution for a 2D dissipative Klein-Gordon equation, J. Math. Anal. Appl. 296 (2004) 286-294.

[51] Maccari A., Solitons trapping for the nonlinear Klein-Gordon equation with an external excitation, Chaos, Solitons and Fractals, 17 (2003) 145-154.

[52] Pang P.H. and Wang M.X., Qualitative analysis of a ratio-dependent predator-prey system with diffusion, Proc. Roy. Soc. Edinburgh Sect. A 133 (2003) 919-942.

[53] Baker R.L., The qualitative analysis of a dynamical system of differential equations arising from the study of multilayer scales on pure metals, Proc. Amer. Math. Soc. 127 (1999) 753-761.

[54] Akuezue H.C., Baker R.L. and Hirsch M.W., The qualitative analysis of a dynamical system modeling the formation of multilayer scales on pure metals, SIAM J. Math. Anal. 25 (1994) 1167-1175.

[55] Clarkson P.A., Nonclassical symmetry reductions of the Boussinesq equation, Solitons in science and engineering: theory and applications, Chaos Solitons Fractals, 5 (1995) 2261-2301.

[56] Bluman G.W. and Kumei S., Symmetries and Differential Equations, Springer-Verlag, New York, 1989.

[57] Stephani H., Differential Equations: Their Solution Using Symmetries, Cambridge University Press, New York, 1989.

[58] Feng Z., Traveling wave solutions and proper solutions to the two-dimensional Burgers-Korteweg-de Vries equation, J. Phys. A (Math. Gen.). 36 (2003) 8817-8829.

[59] Newell A.C. and Whitehead J.A., Finite bandwidth, finite amplitude conviction, J. Fluid Mech. 38 (1969) 279-303.